

Scanning Electron Microscopy for Nanostructure Analysis of Hybrid Multilayer Coating

Debi Rianto

*Department of Physics, Durham University, South Rd, Durham, DH1 3LE, United Kingdom
Corresponding author. Email: debi.rianto@durham.ac.uk*

ABSTRACT

Scanning Electron Microscope (SEM) has been used in various studies to retrieve detailed information on nanomaterial structure. This study is an effort to propose SEM as the proper tool to investigate the properties of Hybrid Multilayer Coating as our model. The analysis should include nanoparticle size and its distribution on the surface, the thickness of the layers, the chemical composition and the crystal grain size in the layers. Several methods in SEM are beneficial to characterize these features are topography image, compositional image, X-Ray Spectrometry and Electron Backscattered Diffraction pattern. This technique also has several limitations ranging from chemical sensitivity, resolution to sample preparation.

Keywords : SEM, nanomaterial, nanostructure



Pillar of Physics is licensed under a Creative Commons Attribution Share Alike 4.0 International License.

I. INTRODUCTION

The microscopy technique is an excellent method for studying and characterizing nanomaterials. In particular, Scanning Electron Microscope (SEM) has been extensively employed in analyzing micro- and nanostructures in many applications. In SEM, an electron beam interacts with the specimen at a specific sample volume, producing various signals to create an image. SEM has a superior resolution than that of a light microscope due to the electron used having a much smaller wavelength than the light has. This tool provides information about the topography and composition of the surfaces by collecting and processing signals generated by a sharp electron probe within a particular interaction volume. Additionally, modern SEM has been already equipped by Energy-Dispersive X-Ray Spectrometry (EDS), enabling users to do chemical analysis. This review provides understanding on fundamental principles of SEM and presenting related sample measurements to investigate the capability of SEM in characterizing the hybrid multilayer structure as our model. The limitations of this method are also considered.

II. THEORITICAL FOUNDATION

A. The Key Principle of SEM

The significant components of SEM are shown in Fig. 1, consisting of an electron gun and electromagnetic lenses, apertures, a vacuum system and a computer or monitor system. The electron gun produces the electron beam and accelerates it at a high voltage of 0.1–40 kV. There are two types of electron guns: tungsten (thermionic gun) and field emission guns. Since the diameter of the electron beam produced by a thermionic gun is too large to form a high-resolution image, in modern SEM, the field emission is preferable as it provides higher current and lowers energy dispersion [1].

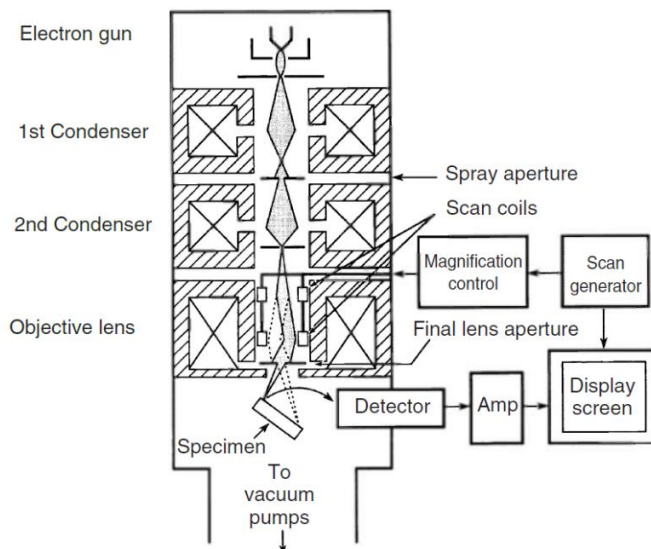


Fig. 1. Scheme of scanning electron microscope instrument [1].

As shown in Fig. 1, there are two types of electromagnetic lenses: a condenser lens and one objective lens. The lenses in SEM are different from that in an optical microscope. The magnetic field produced by wire coils is employed as lenses, and the current applied to the rings can control the trajectories of the electrons along the column. Two condenser lenses converge the electron beam and reduce its diameter, and the objective lens focuses the electron spot on the specimen and supplies further magnification. The aperture in condenser lenses blocks the inhomogeneous and scattered electrons, and the aperture below the objective lens reduces the spot size and enhances the resolution. By this system, the demagnification of the electron beam reach around $10,000\times$ in a thermionic gun and $10-100\times$ in a field emission gun [1]. During the beam-specimen interaction, various signals are produced, which can be used to analyze different types of features. When the beam strikes the specimen, scattering happens between the atoms in the sample and the electron beam, which then deflects the electrons' travel path. Fig. 2 shows the mechanism occurs within a certain depth under the specimen surface.

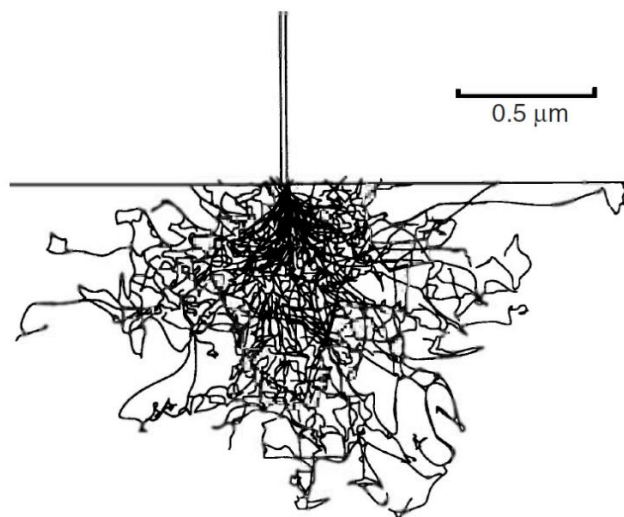


Fig. 2. Schematic electron trajectories in the specimen by Monte Carlo simulation [1].

The beam-specimen interactions can be classified into two major types: elastic and inelastic scatterings. Elastic scattering is a result of a collision of the electron beam by outer shell electrons or with the atomic nucleus of the specimen. During the collision, the energy loss is negligible and backscattered electrons (BSEs) are produced in a wide-angle direction (more than 90°) [2]. On the other hand, the inelastic scattering causes the transfer of energy from the incident beam to the atom, where the amount of the energy depends on the binding energy of the specimen.

The electrons produced during inelastic scattering are called secondary electrons (SE). Both SEs and BSEs contribute to forming SEM images. SEs can escape only from a depth near the specimen surface of 5-50 nm, while BSEs can be detected at depths of about 50-300 nm [1].

Another signal produced during beam-specimen interaction is the characteristic X-rays. The electron beam can break the bond between the inner-shell electron and atom, and the atom is left in an excited state missing an electron in the inner shell. Then, the transition of outer shell electrons filling the internal shell vacancy occurs, which emits a photon. This process is called relaxation. The energy of emitted photon corresponds to the energy difference of transition, which is a specific value for different elements [2]. This Characteristic X-ray can then be used in the elemental analysis of the specimen.

Using these signals, the instrument can construct certain features on the monitor that contain information about the specimen's properties. The elements can be images or spectrums. In a scanning system, probe scanning deflects the electron beam to scan on the surface along the x- or y-axis. The scanning process on the specimen surface is conducted along a line. Then it displaces the probe to a position on the following line for scanning, as shown in Fig. 3, so a rectangular raster is generated on the specimen surface. The signals emitted from the surface are detected by detectors and then amplified and processed on the computer to construct an image [1]. Fig. 3 is an illustration of how the image in SEM is formed. During the scanning, there is a correspondence of one area in a specimen to one pixel on the monitor; the resolution will affect the number of pixels in a monitor. The magnification comes from the ratio of the area scanned on the monitor to the specimen area. Thus, changing magnification means changing the specimen's scanned area as the monitor's size is constant and then providing magnification ranging from 20 \times to greater than 100,000 \times [1].

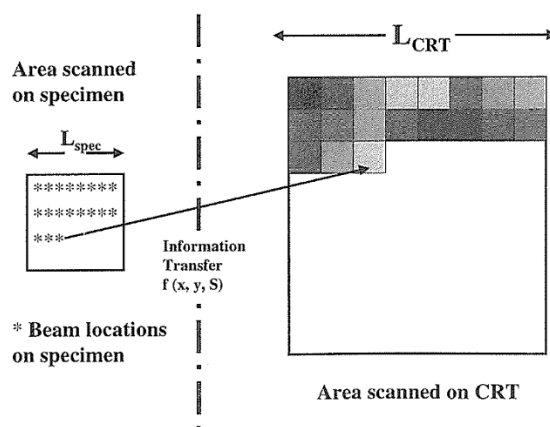


Fig. 3. Schematic of image formation of SEM [2].

B. Modes in SEM

As explained using Fig. 2, some signals are produced during beam-specimen interaction, and every signal can be used to analyze specific properties of the specimen. Different signals will be processed in different modes and produce various features on the monitor. The followings are some modes that are commonly used in SEM.

1) Secondary Electron (SE) Mode

SE mode is usually used to produce topographical images. This is because the SEs can only escape from volume within a few nanometers of the specimen [1] and then give information about the topography of the surface with good resolution. Although some BSEs with directions towards the detectors contribute to topographic contrast, the primary signals are SEs in the contrast formation [1]. The variation of SE signals reaching the sensor will give variation in the monitor's geometric contour and provide information about texture, roughness, particle size, etc.

2) Back Scattered Electron (BSE) mode

As backscattered electrons are produced by the interaction of an atom's outer shell electron, they depend on the atomic number of elements; thus, this signal can create compositional contrast in the SEM images [1]. This characteristic can be explained in Fig. 3. It is notable that the backscattered coefficient increases for greater atomic number of elements. This means that the area with a higher atomic number will produce more BSEs and appear brighter on the images [1].

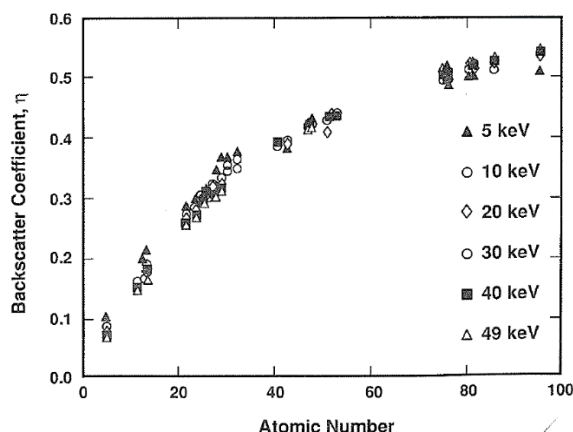


Fig. 4. A plot of the backscatter coefficient against atomic number [2].

3) X-Ray Spectrometry

In modern SEM, chemical elements can be identified by Energy-Dispersive X-Ray Spectrometry (EDS). This can be done by detecting the characteristic X-Ray, which has energy equal to the electron's transition energy difference. Moseley's law defines this energy as the following [1], which gives a relationship between the energy and atomic number.

$$E_{m,n} = R_H(Z - \sigma)^2 \left(\frac{1}{n^2} - \frac{1}{m^2} \right)$$

Where $E_{m,n}$ is the energy of a photon emitted following the relaxation of an electron from the m^{th} to the n^{th} electronic shells in the material of atomic number Z . R_H is the Rydberg unit of energy, 13.61 eV, and σ is a constant that depends on the specific shell. EDS is the most commonly used for microanalysis for examining the chemical composition in a microscopic area [1].

4) Electron Backscatter Diffraction (EBSD)

When the incident electrons reach the specimen surface, the electrons scatter in all directions in a crystalline solid at a certain angle (θ). This is a Bragg scattering. The diffraction pattern provides information about the properties of a crystal. EBSD pattern represents a crystallographic plane indicated by miller indices (hkl). This index can be used to determine the crystal structure and its orientation for each crystal plane. To obtain an EBSD pattern, an acceleration voltage of 10 – 30 kV and beam current of 0.5 – 10 nA in SEM operation produce a probe diameter of 0.2 – 0.5 μm [1].

III. DISCUSSION

A. Designed Structure of Hybrid Multilayer Coating

Fig. 5 is a diagram of the hybrid multilayer structure model potentially used as a coating for metal tools, improving its performance and resistance. Nanoparticles, described by orange shape, composed of 100% element A, are deposited on the surface of the layer. The nanoparticle's size is in the range of 10 – 100 nm diameter and height. The films consist of two different layers repeated N times. The first layer is grown after the metal tools, and its repeated layers (blue layers) are composed of a light element and a heavy element with a ratio of 1:1. The grain size for these layers is in the range of 50 – 100 nm, and the thickness is around 100 nm. On the top of the blue layer, the second type layers are growth, consisting of 90% element B and 10% element C. The films grow around 5 nm thickness and have crystal grains in the 1 – 3 nm range.

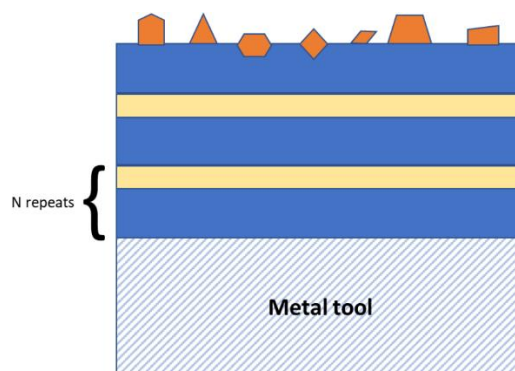


Fig. 5. Schematic of hybrid Multilayer coating model.

The multilayer structure has some parameters that need to be determined to maintain the quality of the coating. Based on the multilayers profile, the analysis should include nanoparticle size and its distribution on the surface, the thickness of repeated layers, the distribution of two different elements in blue layers, the chemical composition of blue and yellow layers and the crystal grain size in the blue and yellow layers.

B. SEM for Analysis of The Multilayer Hybrid Coating.

As explained in the background theory, some modes in SEM operation can be used to investigate specific properties of materials. One of them is the SE image which provides topographical contrast, and further contains information about the roughness, distribution of particles or wires, particle size, etc. As this technique is widely used to determine the nanoparticle profile on the surface, this is suitable for investigating the structure of nanoparticles of element A in the Multilayer Hybrid Coating. To support this claim, several SE images from different studies are provided in Fig. 6.

Fig. 6 shows SE images provide thriving topography contrast for nanoparticles in a different composite structure. Fig. 6.a and 6.b are images of bismuth nanoparticles composited with carbon xerogel. It can be seen that the surface of xerogel is very smooth, which then gives a clear difference between the nanoparticle and gel areas. According to the study in Ref [3], most bismuth nanoparticles have a size of 15 to 250 nm. Gold nanoparticle deposited onto ITO-coated glass substrate, as shown in Fig. 6.c appears to be anisotropic with a diameter distributed from 20 – 150 nm [4]. A high density of Sn nanoparticles was distributed onto graphene as in Fig. 6.d. with a spherical shape, and the particle diameter is 10 – 100 nm [5]. Having some examples of SE images from several nanoparticle studies [3]-[5], it is logical to state that this image would provide significant characterization for A-element nanoparticles on the coating surface. Additionally, based on the multilayer profile, it is expected to obtain a picture similar to Fig. 6.c as the nanoparticles are distributed with low density on the layer surface.

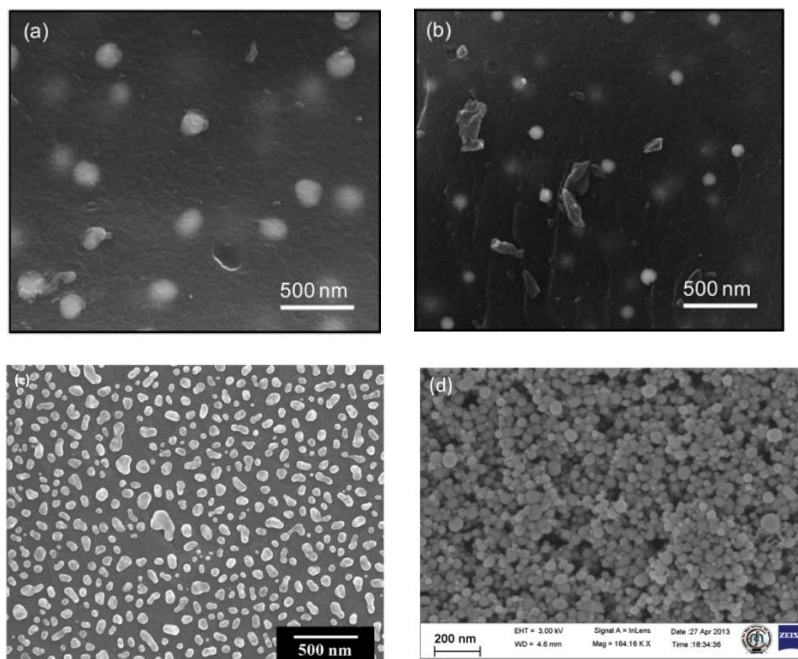


Fig. 6. Secondary electron images of the different structures of materials (a) and (b) carbon xerogel bismuth nanoparticles [3], (c) gold nanoparticle on ITO-Coated substrate glass [4], (d) Sn nanoparticles deposited on graphene nanosheet [5].

However, other things need to be considered in SE images: the effect of electron number and trajectory effect. In the case of edge of nanoparticles, more electrons can escape compared to when the beam hitting the flat surface when the beam strikes the edges of the inclined surface [1]. This causes the edge areas become brighter in the images. We can see this effect in Fig. 6.c in which the edge of gold nanoparticles appears more brighter than other areas. It is vital to observe this effect to gain a more accurate interpretation. Moreover, the variation in how the specimen is oriented to the detector will result in the trajectory effect. Some emitted electrons do not travel in the direction of the detectors, so that the image will appear dark [1].

The blue layers in Fig. 5 are composed of two elements with different atomic numbers: 50% heavy element and 50% light element. We can obtain the compositional contrast images through BSE mode to analyze their distribution on the layer. As explained before, the BSE intensity depends on the atomic number of elements, where the heavy elements will appear brighter on the image and darker for light elements [1]. The study of amalgam/titania nanocomposite [6] showed that amalgam, a metallic alloy, will appear brighter on the BSE image, as shown in Fig. 7, compared with the area composed of titania. This is true because amalgam has a greater atomic number than titania.

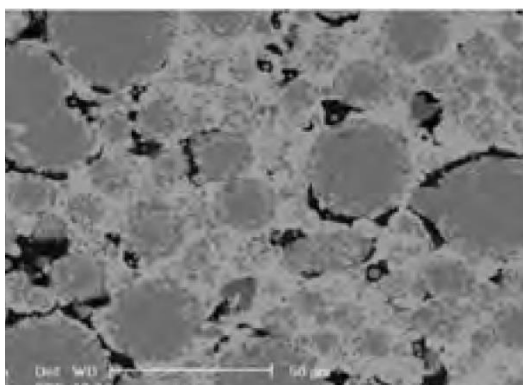


Fig. 7. Backscattered Electron images of amalgam/titania nanocomposite [6].

Despite this, we must consider that the BSE can only be detected in-depth at 50-300 nm [1]. So, the specimen thickness needs to be within that range. As the blue and yellow layers in Fig. 5 will be repeated for N times, according to this escape depth, the maximum N -value will be 2, giving roughly 310 nm total thickness. To overcome this limitation, it is expected to have a cross-sectional image of the coating, which can obtain

compositional contrast for $N > 2$. Fig. 8, as the following, is a BSE image of a multilayer coating cross-sectional area, which signifies the compositional contrast with the coating thickness around 4-10 μm [7].

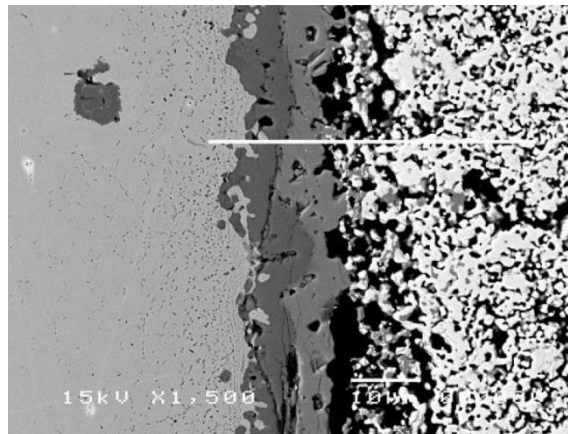


Fig. 8. BSE image of cross-sectional multilayer barrier structure [7].

Although the BSE image could give compositional contrast, this mode could not provide information about what exactly the chemical element on the specimen is. To obtain this specific information, we can use EDS in SEM. X-Ray Spectrometry can identify the chemical composition in blue and yellow layers and the nanoparticle at the surface. An example of an EDS spectrum is quoted from the study of TiO₂ nanoparticles/polypyrrole composite thin films [8], as shown in Fig. 9. The analysis shows that the pure polypyrrole (PPy) thin film comprises 2.03 % C, 18.98% O, 6.81% Al, and 72.18% Ag [8]. By this technique, we can determine the heavy element, the light element, and elements A, B and C on the sample.

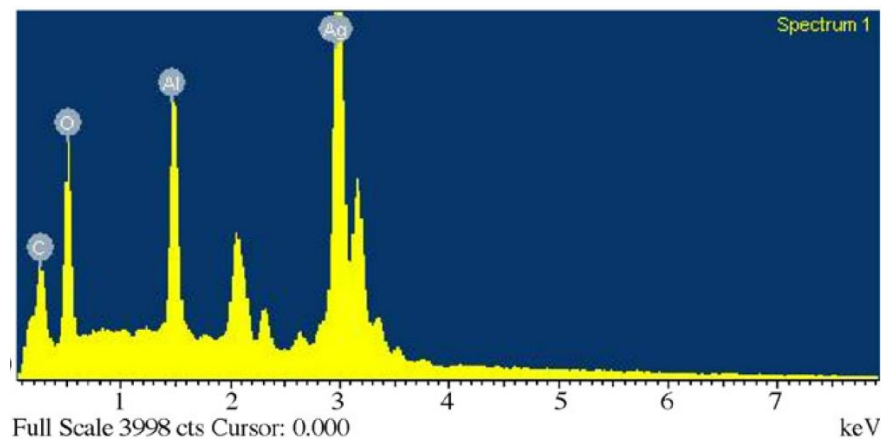


Fig. 9. EDS Spectrum of PPy thin films [8]

Since the resolution of X-Ray signals is relatively slow, the results on the monitors can sometimes be difficult to analyze as there might be overlap between the two lines, such as Mo and S, Ag and Th. This problem can be addressed by performing well polishing in sample preparation to obtain the best signals and applying accelerating voltage twice of energy excitation of the element. Another thing is that EDS in modern SEM is not suitable for macro elements, such as carbon, nitrogen, oxygen, phosphate, sulphur, potassium, calcium, and magnesium [9]. So, another instrument, like inductively coupled plasma mass spectrometry (ICPMS), should be used to analyze these elements.

Further analysis for Multilayer Hybrid Coating is crystal grain size and its orientation. To do this, we can use the Electron Backscatter Diffraction (EBSD) pattern in SEM. This diffraction is looked similar to kikushi pattern obtained by TEM [1], as shown in Fig. 10.a. The analysis requires computer software to indicate the individual zone axis (Fig. 10.b) representing the crystal plane [1]. Based on the pattern, we can also examine the elastic strain of crystal [10], but this is not the scope of this report. Thus, the reader should see a more detailed explanation in Ref [10].

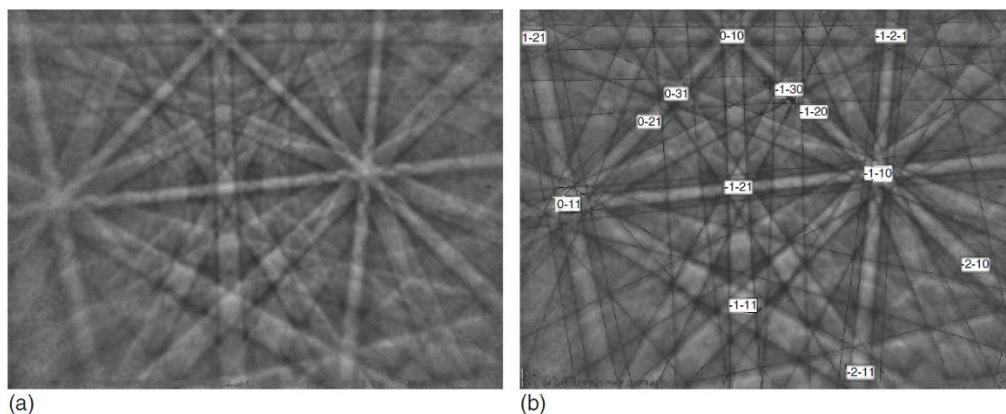


Fig. 10. (a) EBSD pattern of copper, (b) the pattern indexing by computer software [1]

EBSD pattern provides the crystal orientation difference by which we can then identify the grain boundaries and size. Fig. 11.a shows an EBSD map of aluminum alloy where the different orientation among grain is represented by grey levels [11]. The higher the contrast level between the grains, the greater difference in grain angle [1], so we can clearly see the boundaries between individual grains. The grain size distribution is depicted in Fig. 11.c, where the data obtained from 3000 grains, and the average grain size is $0.4 \mu\text{m}$ [11].

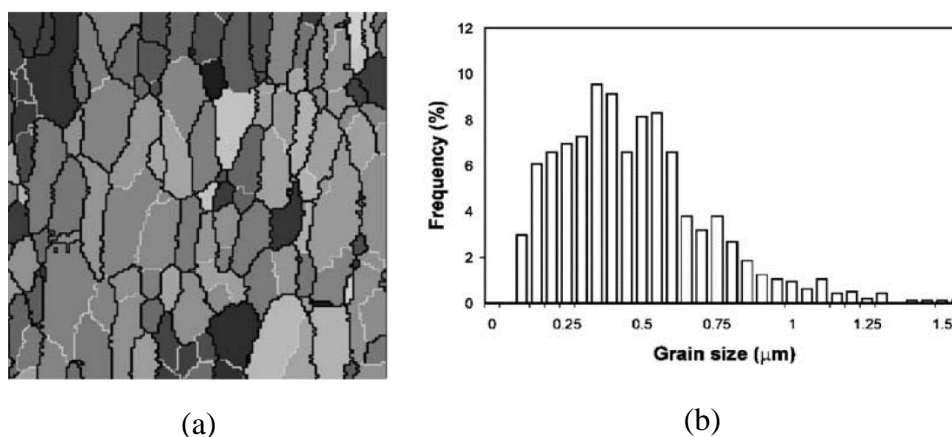


Fig. 11. (a) EBSD image of aluminum alloy and (b) the grain size distribution [11]

Although phase identification can be accomplished with EDS in SEM, we can use EBSD to obtain a more specific phase when a chemical compound has different crystal structures. For instance, TiO_2 generally has three distinct crystal structures: rutile, anatase and brookite [12]. The phase identification in EBSD is similar to X-ray microanalysis. Still, EBSD can identify crystallographic parameters such as crystal plane, angles between planes, and crystal symmetry, providing more specific information about the specified phase.

The cross-sectional SEM image is the most common technique to measure the thickness of layers or thin films. The image in processing software will compare the height of the thin film in pixels and the length of the scale provided on the image. By this method, the thickness of the layers can be determined even on the nanometer scale. To obtain a more accurate measurement, the secondary electron mode would provide a better result for the cross-sectional image as this mode would give geometric contour, for example, the SE image of LMO thin films [13] in Fig. 12.

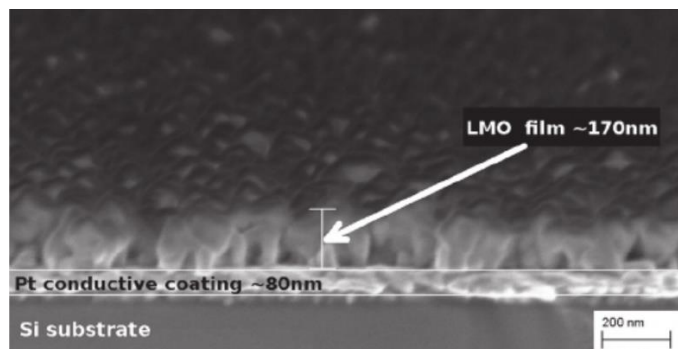


Fig. 12. SEM cross-section image of LMO thin films using secondary electron [13]

Another limitation of SEM is the resolution affected by the probe diameter and current. Minimizing the probe size would result in high resolution and thus, we should increase the brightness and the convergence angles. However, at a certain point, it could introduce spherical aberration. To compensate this effect, minimum probe size cannot avoid optical problems. The probe's current should be larger than the minimum, making it possible to identify microscopic details. However, minimum probe size and maximum probe current could not be obtained simultaneously. Thus, these parameters should be compromised to get the best condition with a high-resolution image in SEM [1]. This resolution will affect how accurate the measurement of nanoparticle size and the thickness of the sample is. According to Tiede et al. [14], the resolution in SEM is 1 nm. However, a study comparing the characterization of SEM, AFM (Atomic Force Microscope), and TEM (Transmission Electron Microscope) concludes that SEM is only suitable for large nanoparticle sizes (above 50 nm diameter) [15]. Since the nanoparticle in our model has the size in the range of 10 – 100 nm, AFM and TEM will perform better than SEM when determining the nanoparticle size [15]. When it comes to thickness, this resolution makes it difficult to measure the thickness of the yellow layers in Fig. 5, which has a size of 5 nm. TEM could be a better alternative for this, but we should consider the thickness of the sample as this instrument requires a very thin model, around 100 nm [1]. We know that the sample has a thickness of more than 300 nm, so it is expected to cut the sample in a cross-sectional area, which further satisfies the sample condition in TEM measurement.

Furthermore, in SEM, most of the samples are solid and have a size that must fit to the specimen holder with a dimension of ten centimeters. Additionally, surface charging indicated by image distortion usually happens in nonconducting samples such as ceramics, polymers, and biological materials. Thus, these samples should be coated with conductive films in the preparation. Specific to topography analysis, we should do a minimum preparation to preserve the surface nanoparticles. Moreover, a sample containing water, usually biological materials, should be prepared with dehydration, which removes the water composition of the materials [1].

IV. CONCLUSION

Scanning Electron Microscope is a valuable technique for analyzing the hybrid multilayer structure. Various modes in SEM will enable scientist to identify the sample's key parameters. The topography contrast will provide an advantage in determining the diameter of nanoparticles and the thickness of layers. The compositional contrast will give information to detect the distribution of different elements in the layers. Moreover, EDS and BSED will provide more detailed information about the chemical composition and crystal structures. Despite some negatives regarding chemical sensitivity, resolution and sample preparation, SEM performs various functionality, which is very useful for the sample model discussed in this paper.

REFERENCES

- [1] Goldstein, J. I., Newbury, D. E., Michael, J. R., Ritchie, N. W., Scott, J. H. J., & Joy, D. C., *Scanning electron microscopy and X-ray microanalysis*, Springer, 2017.
- [2] Leng, Y., *Materials characterisation: introduction to microscopic and spectroscopic methods*, John Wiley & Sons, 2009.
- [3] Gich, M., Fernández-Sánchez, C., Cotet, L. C., Niu, P., & Roig, A, Facile synthesis of porous bismuth-carbon nanocomposites for the sensitive detection of heavy metals, *Journal of Materials Chemistry A*, vol. 1, no. 37, page. 11410-11418, 2013.
- [4] Dou, F., Small, C., Provencher, F., Ferreira, J., Wang, X., Rezasoltani, E., ... & Zhang, X, Particle plasmon-induced charge trapping at heterointerfaces in PCDTBT: PC70BM blends, *Journal of Polymer Science Part B: Polymer Physics*, vol. 55, no. 12, page. 940-947, 2017.

- [5] Thomas, R., Rao, K. Y., & Rao, G. M, Enhanced electrochemical performance of graphene nanosheet thin film anode decorated with tin nanole. *Materials Express*, vol. 4, no. 1, page. 65-71, 2014.
- [6] Bahremandi-Tolou, N., Fathi, M., Monshi, A., Mortazavi, V., & Shirani, F, Preparation and corrosion behavior evaluation of amalgam/titania nano composite, *Dental Research Journal*, vol. 8, no. 5, 2012.
- [7] Nielsen, K., Persson, A., Beeaff, D., Høgh, J., Mikkelsen, L., & Hendriksen, P. V, Initiation and Performance of a Coating for Countering Chromium Poisoning in a SOFC-stack, *ECS Transactions*, vol. 7, no.1, page. 2145-2154, 2007.
- [8] Su, P. G., & Huang, L. N, Humidity sensors based on TiO₂ nanoparticles/polypyrrole composite thin films. *Sensors and Actuators B: Chemical*, vol. 123, no.1, page. 501-507, 2007.
- [9] Erić, S. (2017). The application and limitations of the SEM-EDS method in food and textile technologies. *Advanced Technologies*, 6(2), 5-10.
- [10] Wilkinson, A. J., Meaden, G., & Dingley, D. J. (2006). High-resolution elastic strain measurement from electron backscatter diffraction patterns: New levels of sensitivity. *Ultramicroscopy*, 106(4-5), 307-313.
- [11] Humphreys, F. J. (2004). Characterisation of fine-scale microstructures by electron backscatter diffraction (EBSD). *Scripta materialia*, 51(8), 771-776.
- [12] Zhang, Y., Jiang, Z., Huang, J., Lim, L. Y., Li, W., Deng, J., ... & Chen, Z. (2015). Titanate and titania nanostructured materials for environmental and energy applications: a review. *RSC Advances*, 5(97), 79479-79510.
- [13] Fehse, M., Trócoli, R., Hernández, E., Ventosa, E., Sepúlveda, A., Morata, A., & Tarancón, A. (2018). An innovative multilayer pulsed laser deposition approach for LiMn₂O₄ thin film cathodes. *Thin Solid Films*, 648, 108-112.
- [14] Tiede, K., Boxall, A. B., Tear, S. P., Lewis, J., David, H., & Hassellöv, M. (2008). Detection and characterisation of engineered nanoparticles in food and the environment. *Food additives and contaminants*, 25(7), 795-821.
- [15] Eaton, P., Quaresma, P., Soares, C., Neves, C., de Almeida, M. P., Pereira, E., & West, P. (2017). A direct comparison of experimental methods to measure dimensions of synthetic nanoparticles. *Ultramicroscopy*, 182, 179-190.